Staphylococcal α-Toxin: Formation of the Heptameric Pore Is Partially Cooperative and Proceeds through Multiple Intermediate Stages†

Angela Valeva,* Michael Palmer, and Sucharit Bhakdi

Institute of Medical Microbiology, University of Mainz, Hochhaus am Augustusplatz, D-55101 Mainz, Germany

Received May 8, 1997; Revised Manuscript Received August 13, 1997⊗

ABSTRACT: Staphylococcal α-toxin is a 293 residue polypeptide that assembles into pore-forming heptamers, residues 118−140, thereby inserting to form an amphipathic β-barrel in the lipid bilayer. Fluorometric analyses were here conducted using cysteine-substitution mutants site-specifically-labeled at positions 35 or 130 with the environmentally-sensitive fluorophore acrylodan. In conjunction with functional assays, three conformational states of the heptamer were defined, which may represent transitional configurations of the toxin molecule along its way to membrane insertion and pore formation. The first was the freshly assembled, SDS-sensitive heptamer α_7*a, where a minor alteration in the environment of H35 with no change in the environment of the membrane-inserting stem domain was observed. In transition stage α_7*b, the stem domain moved from a hydrophilic to a more hydrophobic environment, due to protein−protein interaction. Transition to α_7*c involved a cooperative effect, in which residue 35 was forced by a neighboring molecule into a markedly hydrophobic environment. At this stage, the heptamers acquired SDS stability. The final pore conformation α_7 resulted when the stem domain inserted into the lipid bilayer, an event that was driven by H35 within the respective protomer. A model thus evolved in which cooperative forces first lever H35 into a position that subsequently drives the pore-forming sequence within each respective protomer into the membrane. In accord with this model, when hybrid heptamers were formed between a functionally defective H35 substitution mutant and active toxin, only the latter inserted their pore-forming domain into the membrane. In a satisfying functional correlate, pores of reduced size were then generated.

Staphylococcus aureus α-toxin is serving as a prototype for the study of pore formation by proteinaceous toxins in lipid bilayers (*1*). The toxin is secreted as a hydrophilic molecule of 293 amino acids lacking cysteine (*2*), and binds in monomeric form to target membranes. Collision of bound monomers ultimately results in formation of tightly associated heptamers (*3*) surrounding a central transmembrane pore. As an intermediate state, a nonlytic heptamer has been characterized (*4*) that yields the final pore by inserting a centrally located sequence spanning amino acid residues 118−140 into the lipid bilayer (*5*). This region constitutes the major part of what has been termed the stem domain in the recent report on the crystal structure of the α-toxin heptamer (*6*). That work has allowed for assignment of further functional features to parts of the sequence. A rim domain rich in aromatic as well as cationic amino acids and comprising residues 200−260 makes contact with the outer membrane surface. A large cap domain projects to the exterior. Extensive lateral contacts beneath and above the outer membrane plane connect the subunits of the heptamer. One residue involved in such contacts is histidine 35, whose critical role in pore formation has previously been shown by site-directed mutagenesis (*7*, *8*). In those studies, it was demonstrated that replacement of H35 by other amino acids led to total loss of functionality. This defect correlated with the inability of H35R to insert its stem domain into the bilayer (*9*).

The above studies and the crystallographic data have thus revealed that the region surrounding H35 and the stem domain of α-toxin represent two parts in the molecule that assume pivotal functions during pore assembly. The process of oligomerization and pore formation requires that a coordinated series of conformational changes involving protein−protein interactions occur in sequence. To obtain some insight into this process, we have used functionally defective mutants site-specifically-labeled with the environmental reporter molecule acrylodan (*10*) and performed fluorometric and functional analyses on liposomes and erythrocyte membranes. By generating homogeneous and mixed heptamers harboring combinations of functionally intact or defective toxin derivatives, heptamer assembly appeared to be arrested in different conformational stages, and the environment of residues 35 and 130 could be analyzed. Fluorometric measurements were conducted on the heptamers in their membrane-bound and detergent-solubilized state. A change in emission maximum after detergent solubilization was taken to indicate membrane insertion of the labeled residue (*5*). It was found that the first stages of oligomer assembly were driven by cooperative effects, but the final event of stem domain insertion is driven by intraprotomer interactions, with H35 assuming an essential role. When mixed heptamers composed of insertion-defective mutants and wild-type toxin were formed, a reduced number of pore-forming sequences inserted into the bilayer. This led to the creation of channels with smaller functional diameter.

† This study was supported by the Deutsche Forschungsgemeinschaft (SFB 311).

* Corresponding author. Telephone: +6131/17-3128. Fax: +6131/39-2359.

⊗ Abstract published in *Advance ACS Abstracts,* October 15, 1997.

S0006-2960(97)01075-1 CCC: $14.00

MATERIALS AND METHODS

Toxin Preparation. Mutant H35C was recloned from a pT7-derived plasmid (*11*) into pDU1212 (*12*). Wild-type α-toxin and mutant toxins were isolated as described (*5*, *13*). Briefly, the α-toxin-negative *S. aureus* strain DU 1090 (*14*) was transfected with mutant derivatives of pDU1212 and grown in 2*TY broth. Protein from culture supernatants was concentrated by membrane filtration, and the mutant toxins were purified by cation exchange chromatography. Proteins were stored with 5 mM dithiothreitol (DTT) at −70 °C.

Labeling of Sulfhydryl Groups. The mutant proteins were thiol-specifically-labeled with 6-acryloyl-2-(dimethylamino)-naphthalene (acrylodan; both from Molecular Probes, Eugene, OR) or with fluorescein-maleimide as described (*5*, *13*), except that unbound acrylodan was removed by hydroxylapatite chromatography (Bio-Gel HTP; gradient from 20 to 100 mM sodium phosphate, pH 6.8). Removal of unbound label was verified by SDS−PAGE.[1]

Preparation of Liposomes. Egg yolk phosphatidylcholine, egg yolk phosphatidylglycerol, and cholesterol (Fluka; molar ratio 5:1:4) were dried down from chloroform/methanol (2:1 v/v) with N_2 and resuspended to 2 mg/mL total lipid in PBS. Liposomes were prepared by ultrasonication (10 min with a Branson probe sonifier 250, output scale set to 30), centrifuged briefly to remove titanium particles, and used directly.

Preparation of Erythrocyte Ghosts. Five hundred microliters of pelleted rabbit erythrocytes was washed 3 times in PBS and lysed osmotically in 5 mM Tris/HCl, pH 7.5, and the membranes were pelleted by centrifugation (5 min, 10000*g*). They were then repeatedly resuspended in the same buffer and centrifuged until the supernatant remained clear. The membranes were resuspended in 2 mL of PBS. The lipid concentration was determined with an enzymatic cholesterol assay (Boehringer Mannheim), whereby the cholesterol content was divided by 0.3 to yield the total amount of membrane lipids.

Formation of α-Toxin Heptamers. Labeled toxins were incubated with liposomes or erythrocyte membranes (5 μg of toxin per 50 μg of total lipid) for 90 min at 25 °C. To achieve cooligomerization of labeled and unlabeled proteins, these were premixed at the ratios stated under Results prior to addition of liposomes. Where appropriate, oligomerization was confirmed by SDS−PAGE. SDS-sensitive heptamers were detected by gel filtration (see below). To remove unbound toxin, liposomes were collected in a Beckman airfuge (100000*g*, 10 min); erythrocyte membranes were pelleted in a benchtop microfuge (10000*g*, 5 min) and washed twice with PBS. They were resuspended in PBS and analyzed by spectrofluorometry.

Preparation of Delipidated Acrylodan-Labeled α-Toxin Oligomers. Liposomes carrying heptamerized acrylodan-labeled toxin mutants were solubilized with detergent [either 125 mM sodium deoxycholate (DOC) or 2% (v/v) Triton X-100]. To separate oligomers from lipids and residual monomers, the samples were then subjected to gel filtration (15) on a Sephacryl S-300 column, which was equilibrated with 150 mM NaCl, 20 mM Tris, pH 8.3, containing the same detergent in lower concentrations [6.25 mM sodium deoxycholate or 0.1% (v/v) Triton X-100]. Fractions containing the oligomers were collected, checked for heptamer integrity on SDS gels, and used for fluorometry.

Spectrofluorometry. Emission spectra were recorded in a SPEX Fluoromax spectrofluorometer (excitation wavelength: 365 nm for acrylodan, 492 nm for fluorescein-maleimide; band-passes: excitation, 4 nm; emission, 2 nm). The respective buffers and liposome preparations were checked for the absence of significant fluorescence and used as blanks.

Hemolytic titration was carried out as described in (16). To compare the inhibitory effects of the various H35 mutant derivatives, H35R toxin as well as acrylodan-labeled and unlabeled H35RG130C and H35C toxins was mixed with wild-type toxin at equimolar amounts, and the hemolytic titers were compared to that of an equivalent amount of wild-type toxin only. Assays were run in triplicate, and hemolysis was quantitated by measuring the absorbance of the supernatant at 412 nm.

Osmotic Protection Experiments. Rabbit erythrocytes were suspended to 10^9 cells/mL in PBS with 30 mM dextran 4 (M_r 4000). To 1 mL each of this suspension, either 5 μg of wild-type toxin or a mixture of 2.5 μg of H35R and 2.5 μg of wild-type toxin was added. The cells were incubated at 25 °C for 1 h to allow for binding and oligomerization of the toxin. They were then harvested by centrifugation and resuspended in either PBS with or without 100 mM maltotriose (M_r 504). After incubation for 30 min at 37 °C to allow for hemolysis, the samples were subjected to centrifugation, and hemoglobin released into the supernatant was quantitated by measurement of the absorbance at 412 nm.

RESULTS

Functionality of Acrylodan-Labeled α-Toxin Mutant Proteins. The properties of mutants H35R (*5*, *8*), H35RG130C (*9*), H35C (*4*, *17*, *18*), G130C (*19*), and K46C (*5*, *17*) have been described. H35R, H35RG130C, and H35C fully retain cell-binding capacity. They assemble into DOC-stable but SDS-sensitive, nonfunctional oligomers (*4*, *5*, *17*, *18*) wherein the pore-forming domain remains extramembranous. G130C and K46C are fully functional.

The hemolytic activities of mixtures containing equal amounts of wild-type toxin and any one of the labeled or unlabeled H35 mutant proteins were determined by hemolytic titrations at 25 °C. Wild-type α-toxin produced 60% hemolysis of an erythrocyte suspension containing 5×10^8 cells/mL at a concentration of 24 ng/mL, corresponding to 0.72 nM. An equimolar mix of wild-type toxin with any of the inactive mutants produced 60% hemolysis at a protein concentration of 2.9 ± 0.2 nM; i.e., the specific activity of an equimolar mix containing active and inactive toxin was consistently approximately 25% of that of wild-type toxin. It is noted that at those low concentrations leading to 60% hemolysis, the specific binding sites on erythrocytes are not saturated (*21*), so receptor competition should play no role.

K46C α-toxin was prepared and labeled with fluorescein-maleimide (*13*). The labeled toxin fully retained functional activity.

Principle of the Fluorometric Assays. Fluorometric analyses were performed using three labeled toxin mutants: G130Ca is fully active and inserts its stem domain to produce normal channels (*19*); H35Ca and H35RG130Ca are func-

[1] Abbreviations: G130Ca, acrylodan-labeled G130C α-toxin mutant; analogous designations were used for the other mutants; SDS−PAGE, sodium dodecyl sulfate−polyacrylamide gel electrophoresis; DOC, sodium deoxycholate.

tionally defective (*4*, *9*, *17*). These mutants were used to probe the side-chain environment of residues 35 and 130, respectively, in the transition states of the oligomer. A blue shift in the fluorescence emission maximum indicates movement of the fluorophore acrylodan to an apolar environment. Reversal of the blue shift upon delipidation indicates its contact with membrane lipid, whereas lack of blue shift reversal in reisolated heptamers indicates burial of the probe in a hydrophobic protein environment. This conclusion is based on the results of previous experiments that employed a panel of detergents (*5*): the degree of shift reversal is influenced by the detergent used, indicating interaction of the label with detergent and, by inference, with lipid (*20*). In the present study, each analysis of reisolated oligomers was performed in DOC and Triton X-100, and blue shift reversals always followed the same pattern as found previously (*5*). In the following, only the DOC spectra will be shown.

*Prepore Conformational State α_7*a.* The prepore state α_7*a formed when H35Ca was applied to liposomes. A characteristic feature of α_7*a was its sensitivity toward dissociation in SDS, reflecting the fact that tight protomer−protomer interactions had not yet occurred (Figure 1A). Figure 1A shows the acrylodan emission spectra of H35Ca in solution, after its application to liposomes, and after reisolation in detergent. It is seen that oligomer assembly on liposomes was accompanied by only a slight blue shift in the emission maximum of acrylodan attached to H35C, which was not reversed by delipidation. That oligomers had formed was evident from the elution behavior of the reisolated toxin in molecular sieve chromatography, where 85% of H35Ca was recovered in the heptamer fraction (not shown). When the same experiments were conducted with H35RG130Ca, no change whatsoever in the environment of the probe was observed (Figure 1B). By gel chromatography, 92% of H35RG130Ca was recovered in the oligomer fraction (not shown). Thus, α_7*a was defined as a putative early stage in heptamer assembly in which H35 became engaged in protein−protein interactions in the absence of any marked alterations in the organization of the stem domain.

*Prepore Conformational State α_7*b.* This conformational intermediate was detected when the H35RG130Ca and H35Ca mutants were applied to erythrocyte membranes instead of to liposomes. In this case, nonfunctional heptamers assembled that were still SDS-sensitive. However, in addition to the slight environmental change around H35 (Figure 2A), acrylodan attached to residue 130 moved to an apolar environment (Figure 2B). This blue shift was not reversed by delipidation, so it appeared that the stem domain had here been arrested in a hydrophobic protein pocket in transit on its way to the lipid bilayer. It is noteworthy that there was a clear difference in conformation of the stem domain obtained when the same toxin mutant was applied to the two different types of membrane targets. These differences may arise due to differences in lipid composition.

*Prepore Conformational State α_7*c.* This conformational intermediate was detected when the functionally deficient H35Ca mutant was admixed with a 10-fold excess of wild-type toxin (5 μg of H35Ca + 45 μg of wild-type toxin applied to 500 μg of lipid). H35Ca then became incorporated into SDS-stable heptamers, as demonstrable by SDS−PAGE (Figure 3A). In addition to the predominant heptamer band,

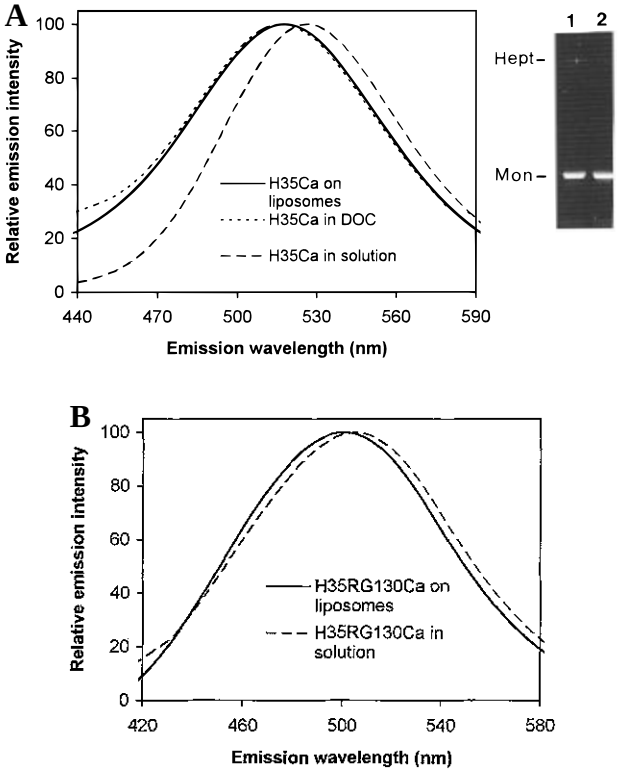

FIGURE 1: Characterization of transition stage α_7*a. Acrylodan-labeled H35C was used to examine the side chain environment of residue 35, and acrylodan-labeled double mutant H35RG130C was used to examine the environmental polarity of residue 130. Transition stage α_7*a was observed when these inactive toxin derivatives were applied to liposomal membranes. (A) Fluorometric analyses of H35Ca as a monomer in solution (λ_{max} = 527 ± 1 nm), as the assembled α_7*a heptamer on membranes (λ_{max} = 516 ± 2 nm), and after reisolation of the heptamers in deoxycholate (λ_{max} = 516 ± 1 nm). Note the small blue shift in emission maximum of the membrane-bound and reisolated membrane heptamers, indicative of movement of residue 35 to a slightly hydrophobic protein pocket. SDS−PAGE of membrane-bound H35Ca (lane 1) and monomeric H35Ca in solution (lane 2) shows that heptamers in this transition stage are dissociated in SDS. (B) Emission spectra of H35RG130Ca in solution (λ_{max} = 507 ± 3 nm), and after heptamer assembly on liposomes (λ_{max} = 502 ± 2 nm). No alteration in the emission maximum was observed, indicating lack of environmental change in the pore-forming domain of the toxin in this transition stage.

two minor bands of low molecular weight were observed. Concomitantly, a pronounced environmental change around residue 35 became apparent (Figure 3A). Detergent solubilization led to partial reversal of this blue shift. This result was surprising because it is known that, in the final pore configuration, H35 is located well outside the bilayer (*6*). α_7*c is characterized by SDS-resistance, indicating that tight hydrophobic protein−protein interactions had occurred (Figure 3A). In accord with this contention, the environment of detergent-solubilized H35Ca in α_7*c was still hydrophobic compared with the monomer and with α_7*a or α_7*b (compare with Figures 1 and 2).

To examine whether the stem domain in an H35 substitution mutant might be coerced via cooperative effects to insert into the membrane, the double mutant H35RG130Ca was employed. When this mutant was admixed with a 10-fold excess of wild-type toxin, however, fluorometry revealed that the reporter molecule did not move into the membrane, and the emission maximum remained unaltered compared with α_7*b. For direct comparison, an experiment with function-

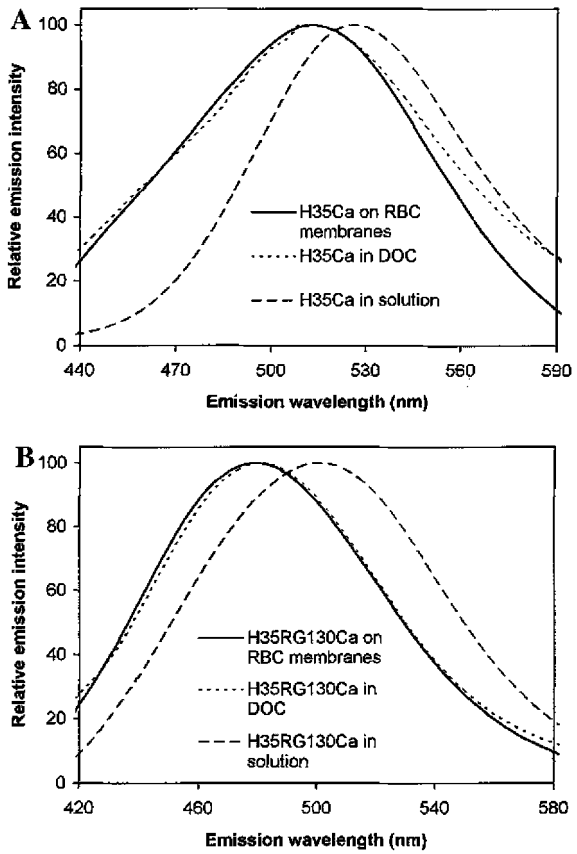

FIGURE 2: Characterization of transition stage α_7*b. This transition stage was observed when the same toxin derivatives used in Figure 1 were applied to erythrocyte membranes. (A) Analyses of H35Ca revealed the same fluorometric findings as observed with liposomes (compare with Figure 1A). (B) In contrast to the situation in liposomes, acrylodan attached to G130C moved to a hydrophobic protein pocket ($\lambda_{max} = 480 \pm 1$ nm); thus, a pronounced blue shift in the emission maximum was observed upon heptamer assembly that could not be reversed by detergent solubilization ($\lambda_{max} = 481 \pm 2$ nm).

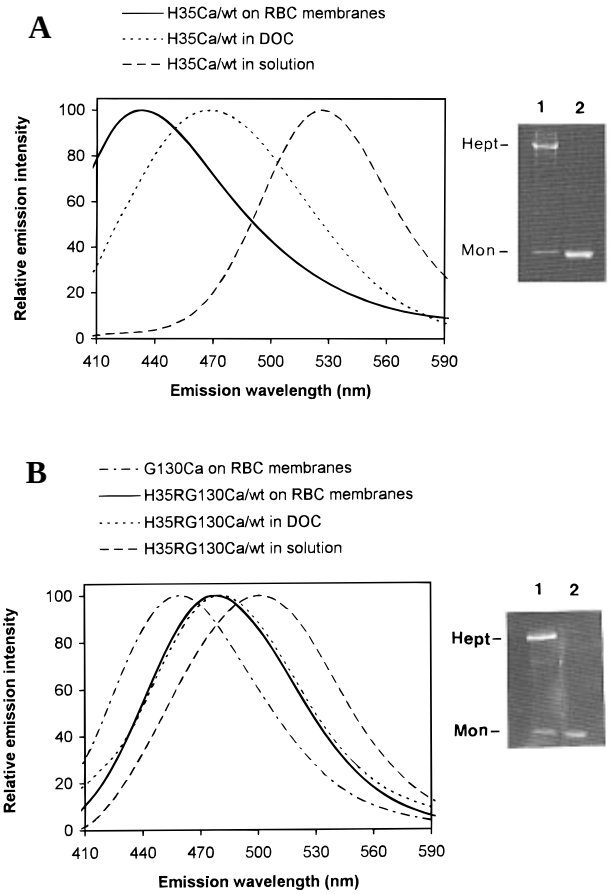

FIGURE 3: Characterization of transition stage α_7*c. This stage was observed when a 10-fold excess of active toxin was added to an H35-inactive mutant. (A) Analyses of the side chain environment of residue 35 in the inactive mutant. Acrylodan was attached to H35C, and the labeled inactive toxin was applied to membranes in the presence of an excess of active, wild-type toxin. Now, co-oligomerization with wild-type toxin led to incorporation of the inactive, acrylodan-labeled derivative into SDS-stable heptamers (lane 1 of SDS−PAGE). As a control, the toxin mix was electrophoresed before addition to the membranes in lane 2. Fluorometric analysis revealed that acrylodan attached to residue 35 experienced a very pronounced blue emission shift upon oligomerization (λ_{max} from 527 ± 1 nm to 435 ± 3 nm). This shift was significantly reversed by delipidation ($\lambda_{max} = 468 \pm 2$ nm). (B) To probe the side chain environment of residue 130 in α_7*c, an analogous experiment was performed whereby acrylodan-labeled H35RG130C was admixed with a 10-fold excess of wild-type toxin. The SDS gel again shows SDS-stable heptamers under these conditions (lane 1; lane 2, native toxin "control"). Here, it was found that the acrylodan moved to a hydrophobic environment upon heptamerization (λ_{max} from 507 ± 3 nm to 480 ± 1 nm), but that delipidation did not reverse this blue shift ($\lambda_{max} = 481 \pm 2$ nm). Hence, the reporter molecule was embedded in a hydrophobic protein pocket. As a control, an experiment is shown in which the functionally intact, single substitution mutant G130C was acrylodan-labeled and similarly used. Here, a blue shift exceeding that observed with the inactive mutant was observed upon heptamerization ($\lambda_{max} = 460 \pm 2$ nm). This blue shift was reversed partially by delipidation ($\lambda_{max} = 481 \pm 1$ nm), yielding an emission spectrum perfectly congruent to that observed with the double mutant.

ally intact G130Ca was performed; note the pronounced blue shift observed in this case (Figure 3B). Thus, α_7*c could be defined as a conformational state at which H35 is driven by cooperative effects into a hydrophobic environment, this correlating with the SDS-resistance of the heptamer, but in which the pore-forming domain has not yet entered the membrane.

Evidence That Inactive H35R Toxin Has an Unaltered Capacity To Form Mixed Heptamers with Active Toxin. At this stage, a crucial question related to the capacity of functionally inactive H35R toxin to associate with active toxin and form mixed heptamers. This issue was addressed with fluorescein-labeled K46C toxin.

According to the crystal structure (*6*), side chains of residue 46 are in quite close proximity to each other in the assembled heptamers. Therefore, it was anticipated that fluorescence quenching would occur when this toxin was specifically labeled with fluorescein and applied alone to membranes. Then, upon addition of unlabeled, active toxin, quenching should be relieved. Figure 4 shows that this is indeed the case: addition of wild-type toxin to fluorescein-labeled K46C toxin dose-dependently enhanced fluorescence. When H35R toxin was applied instead of active toxin, the same results were obtained (Figure 4). These results indicated that there was no significant preference for heptamer incorporation between H35R toxin and wild-type toxin. We thus concluded that formation of mixed heptamers is a random process and that the distribution of the components within the heptamers will be binomial.

Essential Role for Intramolecular H35 for Insertion of the Pore-Forming Sequence. The above results underlined the importance of cooperative interactions for the oligomerization process, but they also revealed that cooperative events alone were insufficient to drive the stem domain into the lipid

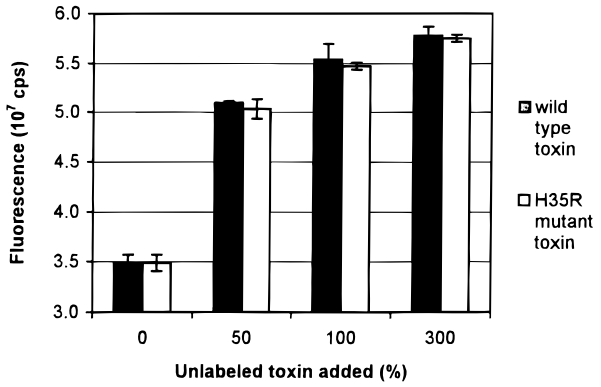

FIGURE 4: Relief of fluorescence quenching indicates comparative incorporation of wild-type toxin and H35R toxin into heptamers. K46C toxin was site-specifically-labeled with fluorecein-maleimide and applied to liposomes in the absence or presence of either wild-type toxin (filled columns) or H35R toxin (open columns). 5 μg of K46C was applied to 150 μg of liposomes in all experiments. Shown are fluorescence measurements obtained in the additional presence of 0, 2.5 μg (50%), 5 μg (100%), and 15 μg (300%) of either wild-type toxin or H35R toxin. The relief of quench indicated comparable replacement of K46C by either wild-type or H35R toxin in the heptamers in all cases.

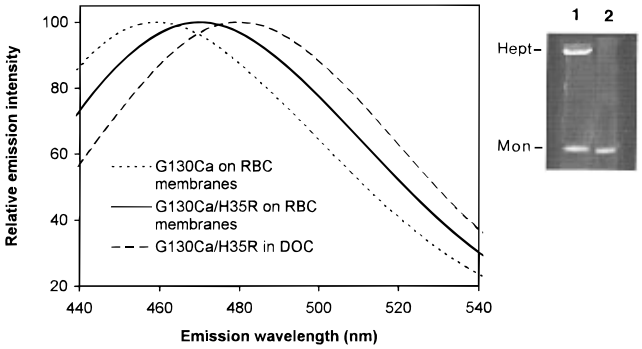

FIGURE 5: Demonstration that acrylodan attached to the functionally intact, single substitution mutant C130C becomes membrane-inserted despite the presence of an inactive H35R toxin mutant within the oligomers. The active, acrylodan-labeled G130C derivative was admixed with H35R toxin in a molar ratio of 1:1. Under these conditions, over 99% of the heptamers should contain at least one H35R molecule. The SDS gel demonstrates that G130Ca/H35R forms mixed oligomers under these experimental conditions (lane 1). Lane 2: native toxin in solution. Shown are the emission spectra of a control, pure G130Ca toxin sample applied to erythrocyte membranes (λ_{max} 460 $\pm$ 2 nm), and the corresponding spectrum obtained with the mixture of G130Ca and H35R (λ_{max} 472 $\pm$ 2 nm). Note that the acrylodan reporter molecule is clearly in a hydrophobic environment in both cases. Upon detergent solubilization, partial shift reversals occurred so that both populations finally yielded the same emission spectra; shown is the spectrum obtained with G130Ca/H35R (λ_{max} 481 $\pm$ 2 nm).

bilayer. By exclusion, this final stage appeared to require intramolecular H35. Should this be the case, then assembly of mixed heptamers harboring insertion-competent toxin (e.g., G130C), and an insertion-incompetent mutant (e.g., H35RG130C), should lead selectively to insertion of the stem domain of the active derivative. This indeed appeared to be the case.

Given an entirely random co-oligomerization of the active and the inactive toxin species, the stoichiometry of the resulting oligomers will be binomially distributed. When applied as an equimolar mix, 98.4% of the G130Ca toxin will become incorporated into oligomers that contain at least one H35R molecule. Now, if a single H35R protomer should be able to prevent membrane insertion of all subunits, the detergent-sensitive blue shift characteristic of the membrane insertion of G130Ca should be virtually abolished. Figure 5 shows that this is not the case, and a blue shift in the fluorescence emission spectrum in the active toxin derivative occurred under these experimental conditions. The blue shift was somewhat blunted compared with that observed with homogeneous G130Ca preparations. Nevertheless, the reversibility of each blue shift by the detergent solubilization indicated that contact with lipid had occurred. Table 1 gives the data obtained in three experiments. From the extent of this reversion (9 nm as compared to 21 nm with pure G130Cac samples), it may be estimated that approximately 50% of the G130Ca molecules had become membrane-inserted in the mixed oligomer preparation under the given condition.

Mixed Heptamers Containing Active and Inactive Protomers Generate Smaller Pores. The above results indicated that in mixed heptamers harboring inactive H35R with active protomers, only the latter insert their stem domain into the membrane. To test whether this might have a functional correlate, osmotic protection experiments were performed. Rabbit erythrocytes were treated with 5 μg/mL wild-type toxin, or with an equimolar mix of 2.5 μg/mL wild-type and 2.5 μg/mL H35R toxin in the preence of dextran as an osmoprotectant. This was done in order to allow oligomers to perform under the same conditions. After 1 h at 25 °C,

Table 1

toxin	λ_{max} (nm) in solution	λ_{max} (nm) on membranes	λ_{max} (nm) DOC solubilized	shift reversal (nm)
G130Ca	512 $\pm$ 1	460 $\pm$ 2	481 $\pm$ 1	21 $\pm$ 2
G130Ca/H35R (mixed 1:1)	512 $\pm$ 1	472 $\pm$ 2	481 $\pm$ 2	9 $\pm$ 2

cells were pelleted and resuspended either in PBS or in PBS + 100 mM maltotriose, and hemolysis was measured after 30 min at 37 °C. As shown in Figure 6, total hemolysis occurred in both cases in PBS. The presence of maltotriose (M_r 504) did not protect cells permeabilized by wild-type toxin, but did offer almost complete protection to cells exposed to the toxin mix, indicating the presence of smaller pores in the latter case. To exclude a possible influence of the maltotriose on the conformation of the mixed oligomers, we also measured the acrylodan emission spectrum of membrane-bound mixed oligomers (G130Ca + H35R) in PBS and in PBS/100 mM maltotriose. The emission spectra were found to be identical (λ_{max} = 472 $\pm$ 2 nm) in both solutions, indicating no direct influence of the maltotriose on the conformation of the stem domain.

DISCUSSION

The three-dimensional structure of the heptameric α-toxin pore has been resolved, and methods to study intermediate steps in pore assembly have been established. Previous work assigned an important functional role to H35 in guiding the oligomerization process. Replacement of H35 by other amino acids did not alter the membrane-binding property of the toxin (*8*, *17*), but assembly to pore-forming heptamers was inhibited, and the H35 mutant protein trapped in prepore oligomers was shown not to insert its stem domain into the membrane (*5*, *9*).

In this study, single and double substitution mutants site-specifically-labeled at residues 35 or 130 with the environ-

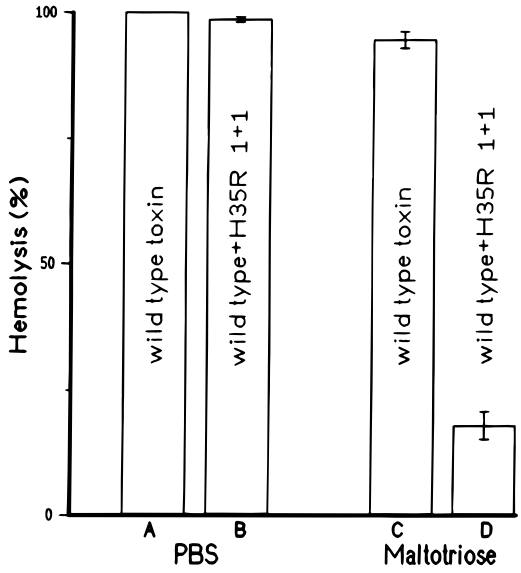

FIGURE 6: Osmo-protection of toxin-treated rabbit erythrocytes. Cells were treated with 5 μg/mL wild-type toxin (columns A, C) or with an equimolar mix of 2.5 μg of wild-type + 2.5 μg of H35R (B, D) in PBS (A, B) or PBS + 100 mM maltotriose (C, D) (see Materials and Methods). Unlysed cells and cell membranes were pelleted by centrifugation, and the absorbance of hemoglobin in the supernatant was read at 412 nm. Maltotriose protected cells from lysis by mixed heptamers (18 ± 2% hemolysis) but not by wild-type toxin oligomers (97 ± 1% hemolysis).

mental probe acrylodan were employed to analyze transition states of α-toxin pore assembly. Prepore conformational states α_7*a to α_7*c were defined as oligomeric configuration states wherein membrane insertion of the stem domain had not occurred. In all these cases, residue 130, which is located at the tip of the membrane-inserting stem domain (*6*), was found not to be in contact with lipid.

The first transition state α_7*a was detected when H35 substitution mutants are applied to liposomes. Then, no environmental change could be observed in the stem domain whatsoever, while the side chain of residue 35 moved to a slightly hydrophobic protein environment. The second transition state α_7*b was characterized by the movement of residue 130 to a hydrophobic protein pocket. This was observed when an H35 substitution mutant was applied to erythrocytes instead of to liposomes. A significant blue shift of the acrylodan emission maximum was then observed that was not reversible after delipidation. The fact that the same toxin derivative displayed different conformations when applied to different membrane targets is noteworthy. With wild-type toxin, indirect indications for such differences have previously been reported in the literature, and they underline the significance of target membrane composition for the pore assembly process (*22*).

In the transition state α_7*c, H35C was forced by neighboring wild-type toxin to a hydrophobic environment. Concomitantly, the heptamers became SDS-resistant. Thus, hydrophobic protein−protein interactions of the N-terminal domain represent an important event along the pathway toward functional pore assembly. This state was detected when H35Ca was applied together with functionally intact toxin to either liposomes or erythrocytes. The location of H35Ca in a hydrophobic environment was remarkable because the blue shift in emission maximum of acrylodan was partially reversed upon delipidation. Previous experiments had shown that such shift reversal reflects contact of the respective side chain with lipid, so we are confronted with the possibility that in α_7*c, H35 contacts the bilayer. Should this be true, this residue must then move out of the membrane during the further steps toward pore formation to assume its final position well outside of the bilayer (*6*). This is, however, speculation, and we cannot exclude hitherto undetected effects of the detergent on the conformation of the prepore.

Several conclusions drawn from the present study require that functional and nonfunctional toxin molecules do interact at random with each other to form mixed heptamers. That the inactive mutants undergo heptamer assembly was clear from previous gel filtration and protease dissection data (*4*, *5*, *17*, *18*). That the inactive mutants became incorporated into mixed heptamers together with active toxin was evident from SDS−PAGE, when an excess of wild-type toxin was applied together with labeled, inactive toxin. In these cases, the bulk of the inactive derivatives became incorporated in SDS-stable heptamers. These findings rendered it legitimate to disregard the minor contribution of any nonoligomerized toxin species toward the overall fluorescence spectra.

The crucial experiment indicating comparable affinity of an inactive H35R toxin for the assembling heptamers involved the analysis of fluorescence quench relief. For these experiments, K46C α-toxin was site-specifically-labeled with fluorescein-maleimide. This mutant was selected because the side chains of residue 46 are located close to one another in the heptamer (*6*) and because it has been shown to tolerate labeling with a large charged reagent without change in function (*17*). The fully functional, labeled K46C molecule must be expected to mix randomly with wild-type toxin. Since the relief of fluorescence quench was identical with H35R and wild-type toxin, we conclude that H35R also co-oligomerizes with active α-toxin entirely at random.

On this premise, the functional data indicate first, that the incorporation of more than two molecules of H35R renders a heptamer functionally inactive. Second, pores formed by heteroheptamers containing one to two H35R must be smaller than those created by wild-type toxin. The first conclusion was derived from the finding that an equimolar mix of H35R and wild-type toxin had 25% functional activity compared to wild-type toxin alone. Given a binomial distribution, 22% of the heptamers will contain one to two molecules of the mutant under these conditions. Loss of 77% hemolytic activity in PBS is thus deduced to derive from those heptamers containing three or more molecules of the mutant. Now, since fluorometric data indicated that only the wild-type toxin inserted its stem domain into the membrane, an intriguing situation arose in which it was envisaged that defective β-barrels formed consisting of a maximum of 10−12 instead of 14 β-strands. To discern whether such defective β-barrels may have a smaller functional diameter, osmoprotection experiments were performed. The results were straightforward: maltotriose did not protect erythrocytes against lysis by wild-type toxin, but afforded almost total protection against lysis by an equimolar toxin mix.

We can envisage two types of defective pore architecture leading to creation of smaller pores. First, inserting amino acid sequences from intact protomers might form a smaller, protein-lined channel. Second, the functionally defective channel might be partially lined by lipid [see model in (*23*)]. The present fluorometric and functional data would be

compatible with both models. Formation of heteropolymers containing insertion-competent and insertion-deficient protomers may emerge as a useful approach for manipulating sizes of toxin pores in experiments that require controlled membrane permeabilization (*24*).

In sum, we have obtained quite detailed information on different conformational states of the α-toxin heptamer, which we believe represent transitional configurations of the toxin molecule along its way to membrane insertion and pore formation. This belief is supported by other lines of evidence. First, the conformational state α_7*b described herein has also been observed on erythrocytes when wild-type α-toxin is applied at 4 °C (unpublished data). Second, we have found that the toxin conformation described as α_7*c is formed when wild-type toxin is applied to certain resistant cells such as granulocytes. In this case, SDS-stable heptamers form in which the stem domain fails to insert into the membrane (*25*), a situation analogous to that found here for conformation state α_7*c. Thus, we believe that the mutants used in this study have revealed true transition states of heptamer assembly rather than deviant dead-end products. The collective data indicate that formation of the heptameric pores is, as expected, partially cooperative, but that the final process of stem domain insertion is driven intramolecularly within each protomer in the assembled prepore.

ACKNOWLEDGMENT

We thank Barbara Walker and Hagan Bayley for providing DNA for mutants H35C and K46C.

REFERENCES

1. Bhakdi, S., and Tranum-Jensen, J. (1991) *Microbiol. Rev. 55*, 733−751.
2. Gray, G. S., and Kehoe, M. (1974) *Infect. Immun. 46*, 615−618.
3. Gouaux, J. E., Braha, P., Hobaugh, M., Song, L., Cheley, S., Shustak, C., and Bayley, H. (1994) *Proc. Natl. Acad. Sci. U.S.A. 91*, 12828−12831.
4. Walker, B., Braha, O., Cheley, S., and Bayley, H. (1995) *Chem. Biol. 2*, 99−105.
5. Valeva, A., Weisser, A., Walker, B., Kehoe, M., Bayley, H., Bhakdi, S., and Palmer, M. (1996) *EMBO J. 15*, 1857−1864.
6. Song, L., Hobaugh, M. R., Shustak, C., Cheley, S., Bayley, H., and Gouaux, J. E. (1996) *Science 274*, 1859−1866.
7. Menzies, B. E., and Kernodle, D. S. (1994) *Infect. Immun. 62*, 1843−1847.
8. Jursch, R., Hildebrand, A., Hobom, G., Tranum-Jensen, J., Ward, R., Kehoe, M., and Bhakdi, S. (1994) *Infect. Immun. 62*, 2249−2256.
9. Valeva, A., Palmer, M., Hilgert, K., Kehoe, M., and Bhakdi, S. (1995) *Biochim. Biophys. Acta 1236*, 213−218.
10. Prendergast, F. G., Meyer, M., Carlson, G. L., Iida, S., and Potter, J. D. (1983) *J. Biol. Chem. 258*, 7541−7544.
11. Walker, B., Krishnasastry, M., Zorn, L., Kasianowicz, J., and Bayley, H. (1992). *J. Biol. Chem. 267*, 10902−10909.
12. Fairweather, N., Kennedy, S., Foster, T. J., Kehoe, M., and Dougan, G. (1983) *Infect. Immun. 41*, 1112−1117.
13. Palmer, M., Jursch, R., Weller, U., Valeva, A., Hilgert, K., Kehoe, M., and Bhakdi, S. (1993) *J. Biol. Chem. 268*, 11959−11962.
14. O'Reilly, M., Azavedo, J. C. S., Kennedy, S., and Fostr, T. J. (1986) *Microb. Pathog. 1*, 125−138.
15. Bhakdi, S., Fuessle, R., and Tranum-Jensen, J. (1981) *Proc. Natl. Acad. Sci. U.S.A. 78*, 5475−5479.
16. Fuessle, R., Bhakdi, S., Sziegoleit, A., Tranum-Jensen, J., Kranz, T., and Wellensiek, H. J. (1981) *J. Cell Biol. 91*, 83−94.
17. Walker, B., and Bayley, H. (1995) *J. Biol. Chem. 270*, 23065−23071.
18. Krishnasastry, M., Walker, B., Braha, O., and Bayley, H. (1994) *FEBS Lett. 356*, 66−71.
19. Ward, R., Palmer, M., Leonard, K., and Bhakdi, S. (1994) *Biochemistry 33*, 7477−7484.
20. Helenius, A., and Simons, K. (1975) *Biochim. Biophys. Acta 415*, 29−79.
21. Hildebrand, A., Pohl, U., and Bhakdi, S. (1991) *J. Biol. Chem. 266*, 17195−17200.
22. Tomita, T., Watanabe, M., and Yasuda, T. (1992) *J. Biol. Chem. 267*, 13391−13397.
23. Bhakdi, S., and Tranum-Jensen, J. (1991) *Immunol. Today 12*, 318−320.
24. Bhakdi, S., Weller, U., Walev, I., Martin, E., Jonas, D., and Palmer, M. (1993) *Med. Microbiol. Immunol. 182*, 167−175.
25. Valeva, A., Walev, I., Pinkernell, M.,Walker, B., Bayley, H., Palmer, M., and Bhakdi, S. (1997) *Proc. Natl. Acad. Sci. U.S.A. 94*, 11607−11611.

BI971075R